Article

Not peer-reviewed version

Electrospun Polylactide – Poly(ε-Caprolactone) Fibers: Structure Characterization and Segmental Dynamic Response

S. G. Karpova , A. A. Olkhov , I. A. Varyan * , O. I. Khan , A.A. Botin , A. V. Naletova , A. A. Popov , A. L. Iordanskii *

Posted Date: 2 April 2024

doi: 10.20944/preprints202404.0063.v1

Keywords: polylactide; polycaprolactone; electrospun fibers; EPR correlation time; amorphous phase, crystalline phase

Article

Electrospun Polylactide—Poly(ε-caprolactone) Fibers: Structure Characterization and Segmental Dynamic Response

S. G. Karpova [1], A. A. Olkhov [1,2,*], I. A. Varyan [1,2,*], O. I. Khan [3,4], A.A. Botin [5], A.V. Naletova [5], A. A. Popov [1,2] and A. L. Iordanskii [4,*]

[1] Department of Biological and Chemical Physics of Polymers, Emanuel Institute of Biochemical Physics, Rus-sian Academy of Sciences, 4 Kosygina street, 119334 Moscow, Russia; karpova@sky.chph.ras.ru (S.G.K.); aolkhov72@yandex.ru (A.A.O.); anatoly.popov@mail.ru (A.A.P.)

[2] Academic Department of Innovational Materials and Technologies Chemistry, Plekhanov Russian University of Economics, 36 Stremyanny lane, 117997 Moscow, Russia; ivetta.varyan@yandex.ru (I.A.V.)

[3] RUDN University, 6 Miklukho-Maklaya St, 117198, Moscow, Russian Federation; oksa_0096@mail.ru (O.I.K.)

[4] N. N. Semenov Federal Research Center for Chemical Physics Academy of Science, 119991 Moscow, Russia; aljordan08@gmail.com (A.L.I.)

[5] Gubkin University, 65 Prospect Leninsky, building 1, 119991 Moscow, Russia; botin-andrey@mail.ru (A.A.B.); naletovaann96@gmail.com (A.V.N.)

* Correspondence: aolkhov72@yandex.ru (A.A.O.), aljordan08@gmail.com (A.L.I.)

Abstract: Electrospun ultrathin fibers based on binary compositions of polylactide (PLA) and poly(ε-caprolactone) (PCL) with different ratios of polymer components from 0/100 to 100/0 wt. % were studied. Using a combination of thermal (DSC) and relaxation (EPR) measurements, the effect of biopolymers content on the characteristics of the crystal structure of PLA and PCL and the diffusive rotational mobility of the stable TEMPO radical in the amorphous regions of PLA/PCL compositions was shown. It was revealed that after PLA and PCL blending, significant changes in the degree of crystallinity of PLA, PCL segmental mobility, sorption capacity of the radical as well as activation energy of rotational diffusion in the amorphous regions of PLA/PCL composition are observed. The characteristic region of biopolymers' composition from 50/50 to 30/70 % PLA/PCL blends ratio was found, where the inversion transition of PLA from dispersive medium to dispersive phase where an inversion transition is assumed when the continuous medium of the PLA transforms into a discrete phase. The performed studies made it possible for the first time to carry out a comprehensive analysis of the effect of the system component ratio on the structural and dynamic characteristics of the PLA/PCL film material at the molecular level.

Keywords: polylactide; polycaprolactone; electrospun fibers; EPR correlation time; amorphous phase; crystalline phase

1. Introduction

To develop environmentally friendly, biocompatible, and bioresorbable, as a rule, bio-based polymers are used which are able to degrade in biological or environmental media under the influence of climatic or biological factors without having the negative effects on living systems and eco-systems [1–4]. Polylactides (PLA) are getting more and more attention because an important feature of such polymers is their macromolecular chain biodegradation by hydrolysis or fermentative hydrolysis. The final products of polymers decomposition are carbon dioxide and water, which are safe for the body [5–7].

Bioresorbable polylactide implants offer advantages in the repair and regeneration of healing tissues, particularly because they are biodegradable and biocompatible. PLA continues to be a suitable material for many medical applications such as tissue engineering, bone fixation devices, and

 doi:10.20944/preprints202404.0063.v1

as a bioresorbable material in orthopaedics and maxillofacial surgery [8,9]. Due to its well-documented biocompatibility, full biodegradability and high stiffness caused by its relatively high temperature of glass transition (Tg), it is used in various industries, including automotive, computer industry, food industry and electrical appliances [10,11]. However, brittleness is a serious disadvantage for the practical application of PLA [12]. At temperatures below Tg, the molecular dynamics in the PCL will significantly differ from the mobility of molecules at temperatures above Tg.

Often a successful approach to softening of brittle or rigid polymeric materials is to add a soft or elastomeric second component by blending. This traditional approach can also be applied to biodegradable polymers for biomedical applications. When the softer component forms a second phase within the more brittle continuous phase, it can act as a stress concentrator, providing a plasticity mechanism and preventing brittle destruction. More recently, PLA has been widely used as a starting material in tabletop filaments for fused sputtering simulation for 3D printers [13].

Poly(ε-caprolactone) (PCL) is a soft, biocompatible and biodegradable semi-crystalline polyester with an elastic amorphous phase at room temperature, since its Tg is about -60 °C and its melting point is in the range 55-70 °C [14]. Aliphatic polyethers such as poly(caprolactone) (PCL) and their copolymers have been shown to be the most commonly used polymers in a wide range of clinical applications: sutures, system drug delivery, coronary stents, fixation screws, etc. This polymer can be biodegraded by external living organisms (bacteria and fungi), but they are not biodegradable in animal and human organisms due to the lack of suitable enzymes [15].

Considering the qualities of all polymers, polycaprolactone polyether (PCL), in addition to being biocompatible and biodegradable, is finding increasing use due to its affordability, cost effectiveness, and suitability for modification. Its regulated physicochemical state, biological properties and mechanical strength allow it to resist physical, chemical and mechanical influences without significant loss of its properties [16–18]. PCL is suitable for controlled drug delivery because of its high permeability for many drugs, excellent biocompatibility and its ability to be completely eliminated from the body after bioresorption. PCL biodegrades slowly compared to other polymers, so it is most suitable for long-term delivery lasting more than 1 year. PCL also has the ability to form compatible mixtures with other polymers that can influence degradation kinetics, facilitating adaptation for achieving desired release profiles [19,20].

The main advantage of combining PLA and PCL is the wide range of properties that can be obtained. One of the main goals of PLA/PCL blends is the development of materials with increased strength while maintaining the biodegradability and biocompatibility of both phases. The low melting point of PCL limits their use in applications where high temperatures are required. However, the softening temperature of products prepared from pure PLA or PLA/PCL mixtures is usually determined by the glass transition temperature of PLA [21–23]. Melting PLA with PCL can reduce the brittleness of PLA, offering a wider range of potential applications.

In [24], they found excellent morphology and remarkable improvements in tensile elongation and impact toughness of the PLA/PCL mixture; in this case, the polymers appeared to have good interfacial adhesion. It was found that incorporation of PCL into the PLA matrix could result in materials with tensile strengths of 18.25 to 63.13 megapascals, Young's modulus of 0.56 to 3.82 gigapascals, strain of 12.65 to 3.27% at maximum strength [25]. Differential scanning calorimetry (DSC) has shown the effect of PCL content on the glass transition temperature (Tg), melting temperature, and degree of crystallinity of PLA/PCL mixtures, when the melting enthalpy of both components of the mixture decreases sharply [26].

It was shown in [27] that, at PCL content up to 20-25 wt %, the mixture has a fine phase structure with small particles and a narrow particle-size distribution. At 30 wt%, the phase structure becomes larger and the particle size distribution expands. At PCL content of more than 40 wt%, the phase morphology becomes continuous. The enthalpy of PLA decreases from 31 to 24 (PLA/PCL=70/30). The strength of the 80/20 PLA/PCL mixture exceeds even the strength of the pure impact-resistant PCL modifier, which meant that there was a synergistic effect. In addition, there is another interesting property of PLA- and PCL-based materials. It is the shape memory effect [28,29]. This specific

 doi:10.20944/preprints202404.0063.v1

behavior consists in the ability of a material to change its original shape when exposed to a specific external stimulus, usually temperature, and to regain its original shape when the stimulus ceases. This change-recovery process can be repeated many times.)

To accelerate the processes of diffusion, hydrolytic destruction and biodegradation, it is necessary to increase the specific surface area of the polymer matrix. From this point of view, film systems are inferior to matrices based on nanoscale and ultrafine polymer fibers. Therapeutic systems, disposable filters, scaffolds and other products based on nonwoven fiber materials obtained by electroforming are currently the most promising and studied objects. The efficiency of these materials is due, on the one hand, to the simple cost-effectiveness of the fiber production technology and, on the other hand, to the possibility of varying the fiber diameter in a wide range (from 100 nm to 10 μm) [30]. The processes of bioresorption, oxidation and hydrolysis are significantly affected not only by the morphology of the fibrous material, but also by the structure of the elementary fiber [31]. The rate of these processes increases if the fiber structure is heterogeneous. The most heterogeneous structures have formed by blending of polymers, which, as a rule, are thermodynamically incompatible [32]. Polymers in blends exert mutual influence on the processes of crystallization, glass transition, leading to an increase in diffusion-transport characteristics [33], acceleration of the kinetics of bioresorption, oxidation and photo-oxidation of composite fibers [34].

At room temperature and body temperature, PCL exhibits low tensile modulus (E 400 MPa) and high relative elongation rupture (400%). On the contrary, PLA at room temperature and body temperature exhibits high modulus of elasticity and low elongation at rupture (E=3-4 Gpa). Often, unless there is a favorable specific interaction between the components, miscibility is very rare and is detected only when the solubility parameters match each other. This is the case for PLA/PCL mixtures; the mismatch between solubility parameters is small (10.1 (cal/cm^3) for PLA vs. 9.2 (cal/cm^3) for PCL. For mixtures that are immiscible, the most fundamental question concerns phase morphology and the structure of interfacial interlayers. It was shown in that the PLA/PCL systems are phase-separated, but they are not completely immiscible, since the PLA-rich phase partially dissolves the PCL. Differential scanning calorimetry and dynamic mechanical analysis (DMA) of PLA/PCL mixtures showed the presence of two Tg at positions close to the pure components, indicating phase separation. However, the shift in the position of the tan δ peak on the DMA from 64 to 57°C suggests partial solubility of PCL in the PLA-rich phase. In [23] it was concluded that PCL prevents the crystallization of PLA

Currently, functional carriers of biologically active compounds and absorbents with high specific surface area are widely used in biomedicine in the form of bioceramic materials, polymeric therapeutic systems, framework structures for cell engineering, nanoscale hybrid means of directed drug transport, and a number of other innovative systems that simultaneously fulfil the functions of implants and carriers of biologically active compounds [35–37]. The greatest practical and commercial advantages are found in composite ultrathin fibres [39,40], which have high specific surface area, structural diversity and the ability to effectively control drug delivery. Obtaining polymeric modifications of biologically active compounds is an actively developing branch of chemical technology and is aimed at the synthesis of polymeric materials with significant biomedical properties.

One of the advanced methods for producing ultrafine fibres is electrostatic forming or electroforming of polymer solution (EF). The main advantages of EF include relatively low cost of equipment and simplicity of tooling, variability of conditions for fibre obtaining, as well as a variety of different types of fibres and products based on them [35]. The use of a number of natural polymers, such as poly-(3-hydroxybutyrate) and polylactide creates additional advantages in the development of fibre and matrix systems for environmental applications and in biomedicine. Fibrillar matrices and mats formed by nanofibres create favourable conditions for free migration and proliferation of cells in the three-dimensional space of framework structures, and, accordingly, provide high integration affinity of the material to living tissues of the organism [41]. They are actively used in the design of biosensors, nanofilters, for wound therapy, for the immobilisation of enzymes, for the creation of

 doi:10.20944/preprints202404.0063.v1

prolonged and targeted means of drug delivery and in other areas of modern biology and medicine [42].

In the works devoted to the study of the structure and properties of PLA/PCL mixtures the data on the crystal structure are given, but there are no works on studying the structure of amorphous regions. The structure of amorphous phase in blended compositions is also of interest. Therefore, the aim of this work is to study the structure formation of nonwoven fiber materials based on mixtures of polylactide and polycaprolactone, obtained by electroforming.

2. Materials and Methods

We used natural polylactide (PLA) of NatureWorks® Ingeo™ 3801X Injection Grade PLA (SONGHAN Plastics Technology Co., Ltd.) brand with an average viscosity molecular weight of 1.9 × 105 and Polyε-caprolactone pellets (Mw~80,000, Sigma-Aldrich) polycaprolactone (PCL), melting temperature 60 °C.

Ultra-thin PLA/PCL fibers were produced by electroforming [43] using a single-capillary unit (Russia, Moscow). Capillary diameter is 0.2 mm. The distance between the capillary and the precipitation electrode was 20 cm. Voltage was 17 kV. Moulding solutions of PLA/PCL in chloroform were prepared at different polymer ratios. The total concentration of polymers in the solution was 7 wt%. Stirring was carried out using an automatic magnetic stirrer at 50 °C.

EPR spectra (X-band) were recorded on an automated spectrometer EPR-B (Institute of Chemical Physics, Russian Academy of Sciences). The value of microwave power in the resonator did not exceed 7 mW, what allowed to avoid saturation effects. When recording spectra, the modulation amplitude was always significantly less than the resonance line width and did not exceed 0.5 Gs. The stable nitroxyl radical TEMPO served as a probe. The radical was introduced into the fibers from vapor at 50 and 70°C. The concentration of the radical in the polymer did not exceed 10-3 mol/L. The experimental spectra of the spin probe in the region of slow motions (probe rotation correlation time $\tau > 10\text{-}9$ s) were analyzed within the isotropic Brownian rotation model according to the program described in [44].

When modeling the spectra, the following principal values of the g-tensor and the radical superfine interaction tensor were used: $g_{xx} = 2.0096$, $g_{yy} = 2.0066$, $g_{zz} = 2.0025$, $A_{xx} = 7.0$ Gs, $A_{yy} = 5.0$ Gs, $A_{zz} = 35.0$ Gs. Note that the value of A_{zz} was determined experimentally from the EPR spectra of the nitroxyl radical in the polymer at 77 K; it did not differ significantly from the value given in [45]. The probe rotation correlation times τ in the region of fast rotations ($5 \times 10^{-11} < \tau < 10^{-9}$ s) were found from the EPR spectra by the formula [46]:

$$\tau = \Delta H^{+} [(I^{+}/I^{-})^{0.5} - 1] 6.65 \times 10^{-10} \quad (1)$$

where ΔH^{+} – width of the spectrum component located in the weak field, I^{+}/I^{-} - ratio of intensities of the components in the weak and strong field, respectively. The measurement error τ was ±5%.

The equilibrium concentration of the adsorbed radical in the samples of the studied compositions of the same mass was calculated using Brucker (Winer) software. In the process of taking spectra, the amplification was recorded, the sample was weighed, and then the calculation of the radical concentration in each sample was made in the Origin program.

The samples were investigated by the DSC method using the NETSZCH STA 449 F5 Jupiter. 50-70 mg of the sample was loaded into a corundum crucible and heated in a stream of nitrogen at a flow rate of 100 ml/min in the temperature range from 20 to 250 degrees at a rate of 2 degrees per minute.

The morphology of nonwoven samples was studied using laser scanning 3D microscope LEXT OLS 4100. The method consisted in the fact that the sample was fixed on a cover slip and placed on the microscope stage: then the area of the surface and the required magnification were selected, the focus was adjusted, and the image was taken. Microphotographs were processed using a standard software package.

Preprints.org (www.preprints.org) | NOT PEER-REVIEWED | Posted: 2 April 2024 doi:10.20944/preprints202404.0063.v1

3. Results

3.1. PLA/PCL Fiber Geometry

Figure 1 shows microphotographs of nonwoven fiber materials PLA-PCL. Fibers based on polymer blends have multiple thickenings in the form of beads. The size of the thickenings varies from 10 to 40 μm.

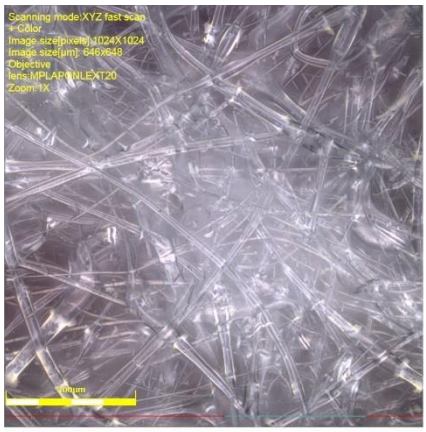

(a)

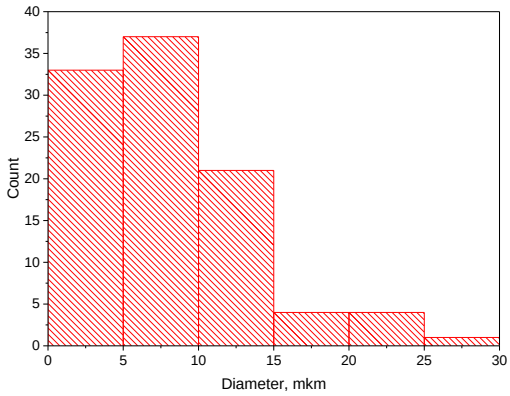

(a1)

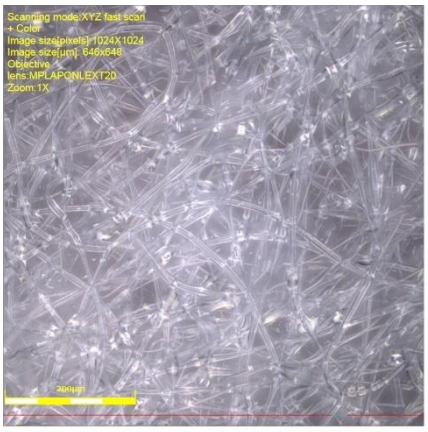

(b)

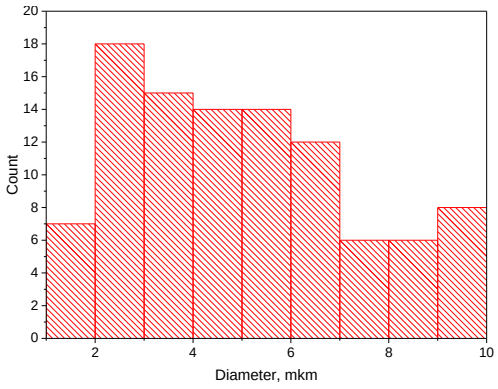

(b1)

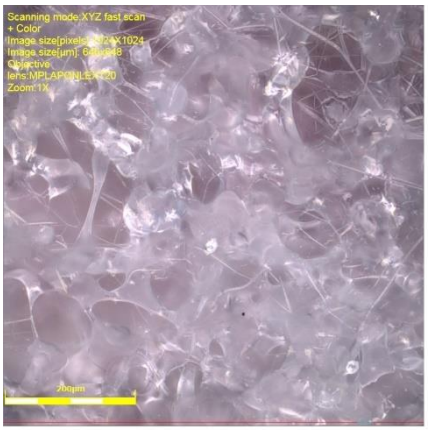

(c)

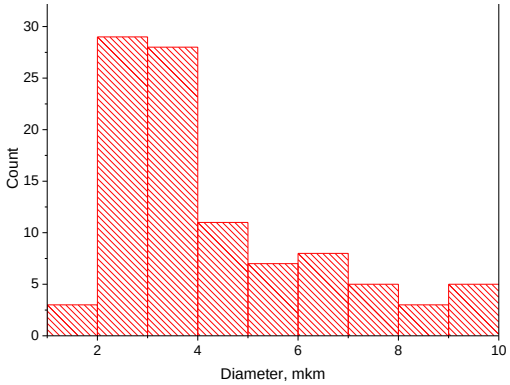

(c1)

Preprints.org (www.preprints.org) | NOT PEER-REVIEWED | Posted: 2 April 2024 doi:10.20944/preprints202404.0063.v1

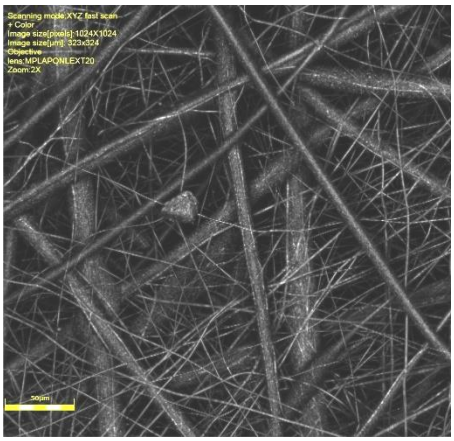

(d)

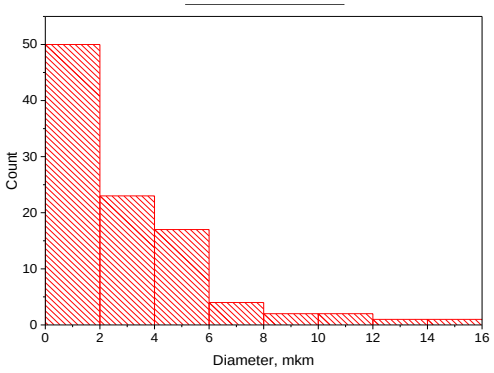

(d1)

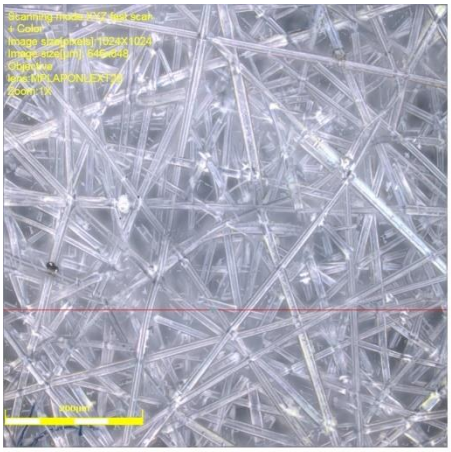

(e)

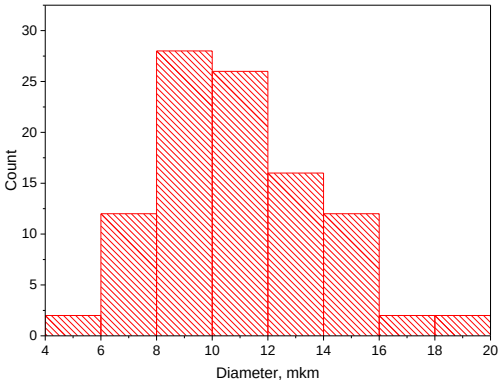

(e1)

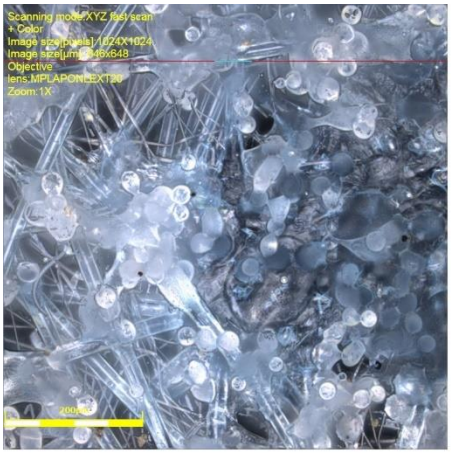

(f)

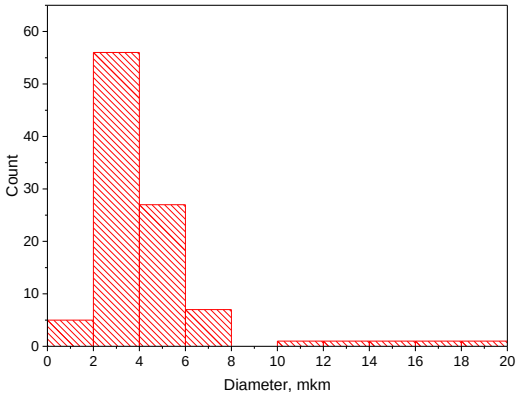

(f1)

Preprints.org (www.preprints.org) | NOT PEER-REVIEWED | Posted: 2 April 2024 doi:10.20944/preprints202404.0063.v1

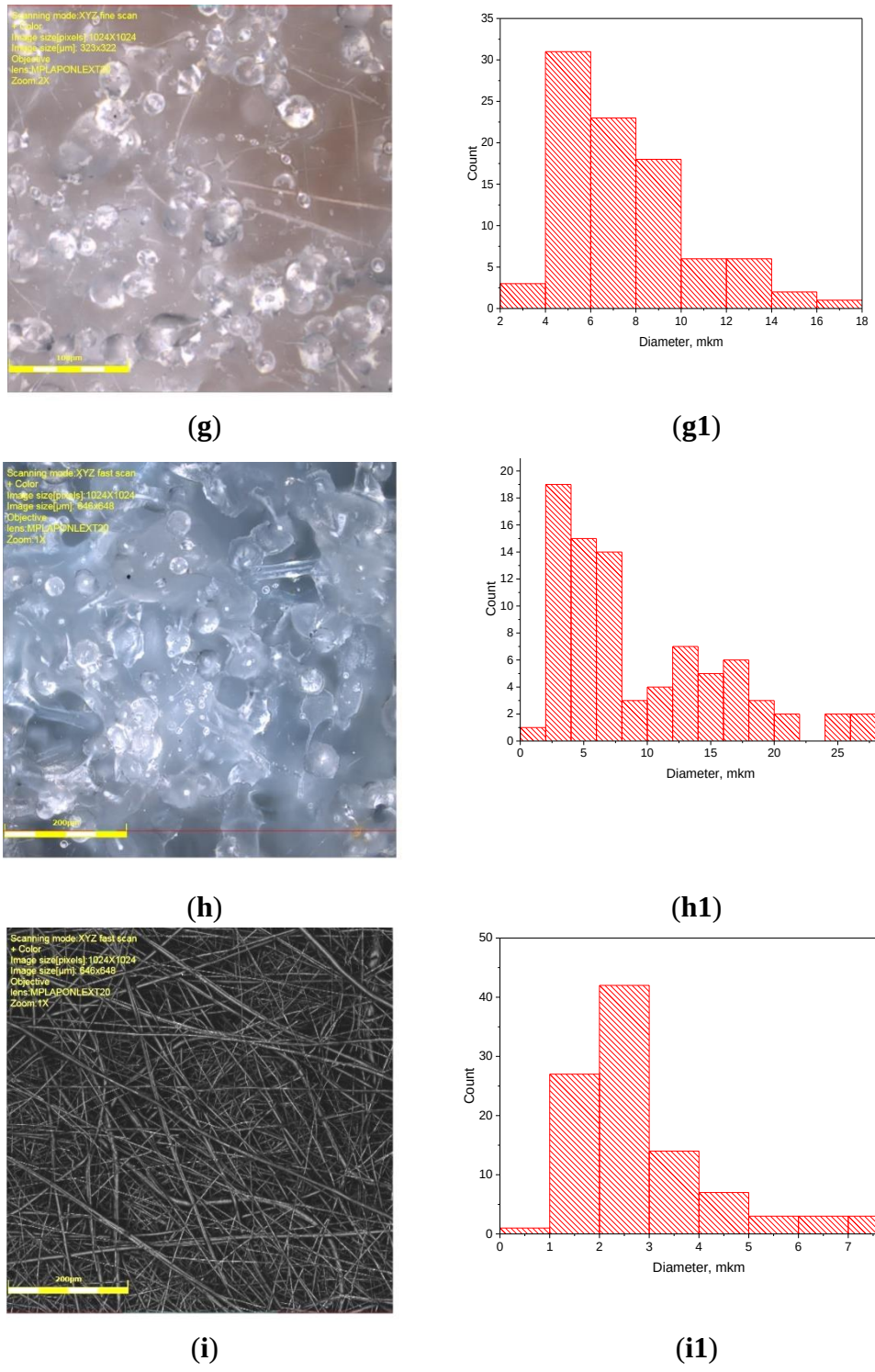

Figure 1. Microphotographs of PLA-PCL fiber materials: 100-0 (A); 90-10 (B); 80-20 (C); 70-30 (D); 50-50 (E); 30-70 (F); 20-80 (G); 10-90 (H); 0-100 wt% (I). The right column shows the corresponding histograms of fiber diameter distribution.

The cause of thickening is related to rheological features of PLA and PCL in the blends. The tensile dynamics of polymer solutions seems to be complicated by relaxation processes in polymer phases at the interface and different values of surface tension due to the molecular characteristics of polymers. This is evidenced by values of diameters of individual polymers: PLA fibers have diameter of 5-15 μm, and PCL 2-5 μm (Figure 1a, I, respectively). The values of cylindrical fibers diameters in PLA-PCL mixtures lie in the range of 2-12 μm. Large variation in the values of mixture fibers diameters is due to the processes of splitting of the primary jet and unsteady rheological behavior of

 doi:10.20944/preprints202404.0063.v1

binary mixtures during capillary passage and pulling of the solution drop in the field of electrostatic and hydrodynamic forces. We should pay attention to the morphology of fibers based on PLA-PCL blend: 50-50 wt.%. They have an even cylindrical shape and have practically no thickenings. Apparently, it is connected with formation of structure from two continuous phases while at other ratios one of polymers in mixture acts as disperse phase and at formation of a jet tends to coagulation and formation of drops. It is quite possible that the level of intermolecular interaction between PLA and PCL influences the process of formation of the blended fiber geometry. Based on the analysis of the morphology of blended fibers, we can assume a rather low level of interaction between PLA and PCL. However, to confirm or refute these conclusions, it is necessary to conduct a structural-dynamic analysis of the crystalline and amorphous regions in the blended fibers.

3.2. Thermal Characteristics of PLA/PCL Binary Fiber Composition

The processes of biodegradation, oxidation and hydrolysis are significantly affected not only by the surface morphology of the film or fiber material, but also by the structural organization of the amorphous and crystalline phases formed in the composite volume [47–49]. Polymers in mixtures have mutual influence on crystallization processes. Let's consider influence of addition of PCL to PLA on crystalline structure of blended compositions.

In the process of mixing of two polymers (PLA, PCL) along with the change of morphology of ultrafine fibers one should expect changes in their thermophysical and structural characteristics. DSC method was used to study thermophysical characteristics of the fibers. For this purpose, thermograms of PLA and PCL fibers and their blended compositions were obtained.

Figure 2 shows the heating peaks of PLA (a) and PCL (b). The DSC curves of polymer samples of different composition with component ratio from 100/0 to 50/50 % PLA/PCL showed 3 characteristic peaks: two endothermic peaks and one exo-peak. A characteristic feature of these thermograms is the overlapping of endothermic peaks of melting of PCL and glass transition of PLA, which complicates the calculation of the enthalpy of melting of PCL. The presence of exopeak at 85.95 ºC in PLA indicates the process of cold crystallization and formation of linear structures in the fibers, which indicates the presence of a large proportion of straightened chains in the polymer, which are characterized by a large entanglement at temperatures below 85.95 ºC. At higher temperatures, there appears the possibility to form crystalline and linear structures.

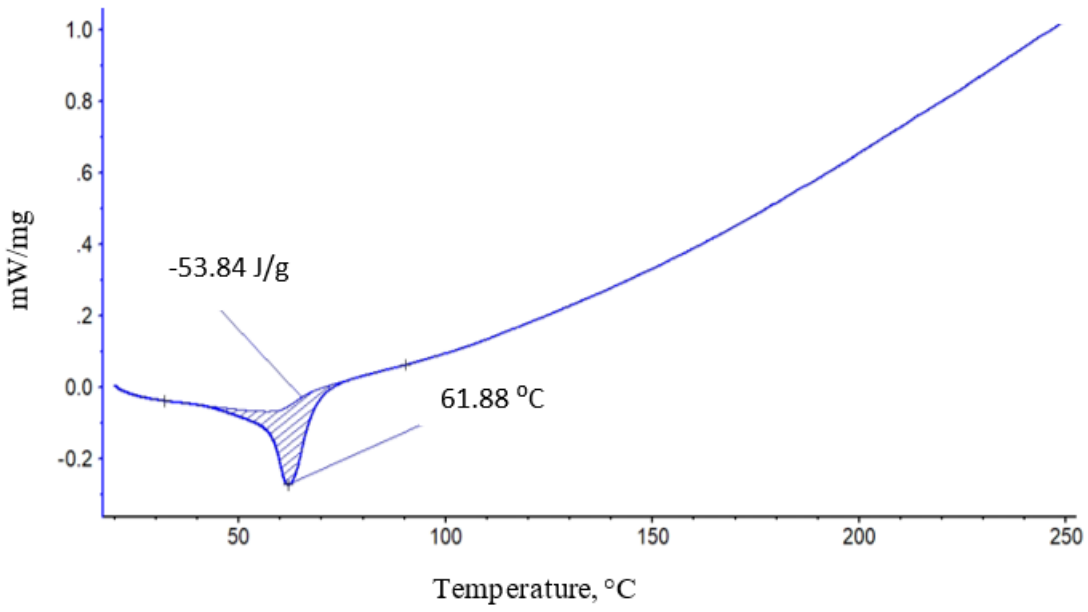

(a)

 doi:10.20944/preprints202404.0063.v1

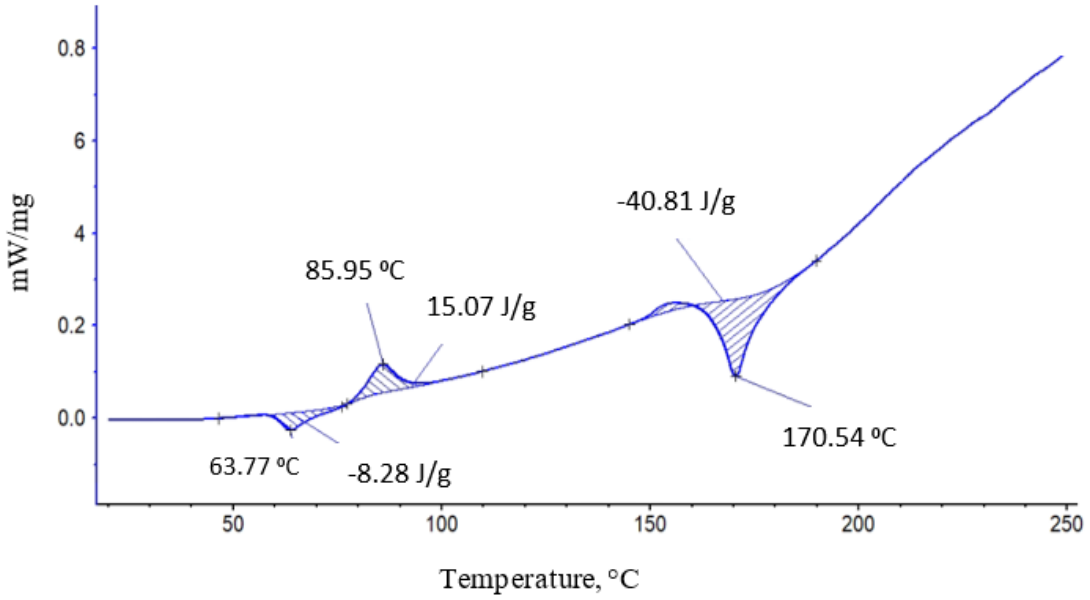

(**b**)

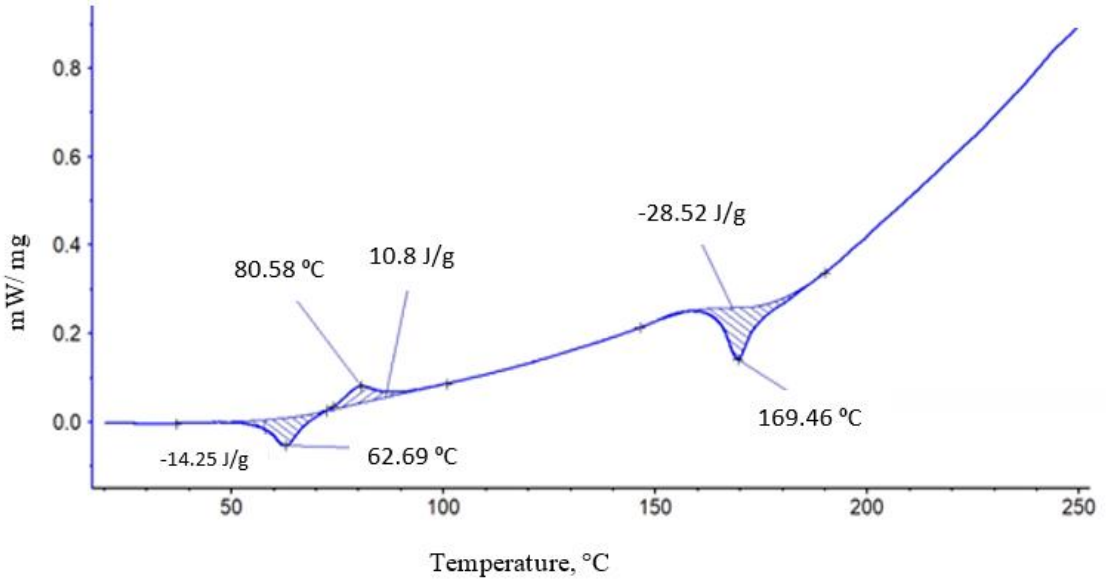

(**c**)

Figure 2. Thermograms of melting of initial PCL (**a**), PLA (**b**), PCL/ PLA 50/50 (**c**).

With the addition of 10 % PCL, the enthalpy of melting of PLA increases dramatically (Figure 3) to the highest value. It can be assumed that the first portion of PCL is distributed in the system in the form of tiny particles, thereby plasticizing the structure of PLA and, as a result, the proportion of straightened chains increases sharply, ΔH increases almost 4 times relative to the initial PCL crystallinity.

 doi:10.20944/preprints202404.0063.v1

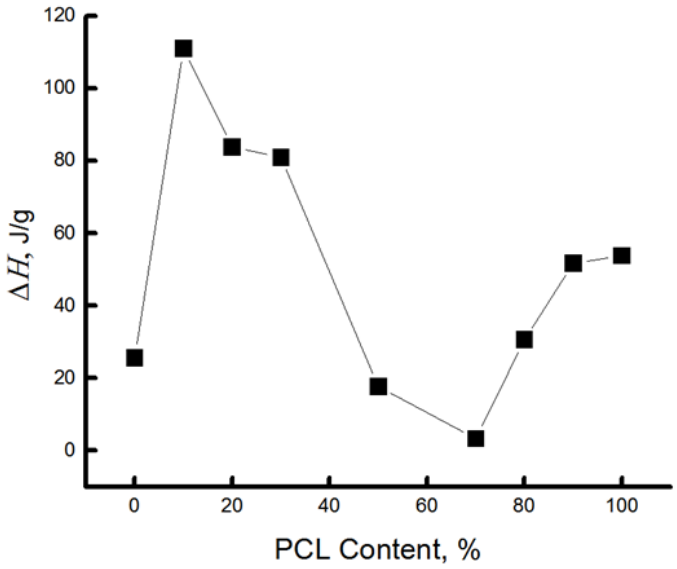

Figure 3. Dependence of ΔH on fiber composition.

It can be assumed that the growth of melting enthalpy is also affected by additional crystallization on PCL particles, probably at the small addition, its particles are the centers of crystallization. At the same time, the enthalpy of cold crystallization of PLA decreases sharply (2-fold). It was shown in [23] that at PCL content up to 20-25 wt %, the mixture has a thin phase structure with small particles and a narrow particle-size distribution. At 30 wt. %, the content of dispersive phase structure enlarges and the particle size distribution expands. At PCL content of more than 40 wt %, the morphology of the phases becomes continuous, with the PLA-rich phase partially dissolving the PCL. With increasing concentration of PCL, ΔH begins to decrease, apparently, the particle size distribution expands, the effect of plasticization and additional crystallization begins to decrease.

Now let's consider the change of enthalpy of melting of PCL. The complexity of calculating of this parameter consists in superimposing of the PCL melting peak (T_m=62 ºC) and the PLA glass transition peak (T_{gt}=64 ºC) on the thermogram. However, the total value of ΔH can be used to estimate the change in the melting enthalpy of PCL when mixed with PLA. Table 1 shows that when PCL is added to the mixed composition up to and including 70%, its ΔH is extremely low, i.e., the proportion of crystallites and linear systems in PCL is negligible.

Table 1. Enthalpy and temperature of melting, cold crystallization, glass transition of nonwoven fiber materials PLA/PCL according to DSC data.

PCL content in the mixture, %	***ΔHcr.*, J/g**	***T*melt, °C**	***T*gt, °C**	***ΔHcc*, J/g**	***T*melt, °C**
0	25,7	170,54	63,77	-15,07	86
10	111	170,1	63,3	-10,7	82,3
20	83,8	170,1	63	-8,1	80,8
30	82	170	63	-5	80,1
50	17,7	169,5	62,7	-3,5	78
70	3,36	167,9	62		
80	30,6	167,5	61,6		
90	51,7	165,1	61,4		
100	53,84	61,8	61		

 doi:10.20944/preprints202404.0063.v1

The results confirm the conclusion about the fine-dispersed distribution of PCL in the PLA matrix when it is added to the mixture up to 70%. And only starting from the 30/70 % PLA/PCL composition, when polycaprolactone forms a continuous phase, the formation of crystallites and linear systems of PCL occurs in the mixture, the proportion of which increases significantly with increasing concentration of the latter in the mixture (Table 1).

Let us point out the reason for spontaneous straightening and additional orientation of the chains. It is known from thermodynamics that the conformational criterion k*= h/L (where h is the average distance between chain ends and L is the contour chain length) determines the tendency of a macromolecule to straightening and additional orientation or to folding into a ball. Each polymer has its own critical value k*. Chains with k>k* tend to additional orientation, macromolecules with k<k* tend to take a ball conformation. Therefore, a certain portion of straightened macromolecules is formed in the process of fiber production, however, the system does not fully assume an equilibrium state during molding and recrystallization with growth of crystallite sizes and the portion of straightened chains in the amorphous phase occurs during structure loosening (in this case by PCL particles). Isothermal thickening of longitudinal dimensions of crystallites occurs due to movement of the fold as a whole through the crystal, and also as a result of straightening of sufficiently straightened chains in inter-fibrillar and intrafibrillar regions. In this case the structure of amorphous regions also changes.

The nature of changes in the thermal characteristics of the binary PLA/PCL system depending on the composition of polymer components allows us to draw a preliminary conclusion that there is a certain region of concentrations from 50/50 and 30/70 % of PLA/PCL where phase inversion takes place, i.e., when the continuous (dispersed) phase of PLA transforms into dispersed phase. In this concentration range, the enthalpy of melting of PLA and PCL is characterized by very low values, there are no exo-peaks characteristic of PLA, and there is a kink in the dependence of ΔH on composition (Figure 3).

The addition of small concentrations of PCL into the system promotes the formation of a certain fraction of more perfect crystallites with a melting point of about 220 ºC (the melting range lies between 160 and 220 ºC), while in the original PLA this range lies between 160 and 190 ºC. Note that the melting enthalpy data obtained by the DSC method provide information on both the fraction of crystalline phase and linear structures (structures made of straightened chains with a two-dimensional order) in the fiber.

With an increase in the concentration of PCL over 70% in the system, the enthalpy of melting of both PLA and PCL increases sharply (Table 1). In the region of compositions with 80-90% PCL content the enthalpy of melting of this polymer is 33.6 and 33, 8 J/g, while in the homopolymer is 54 J/g. It can be assumed that at these compositions interfacial layers are formed, which partially prevent the formation of the crystalline phase.

Thus, the study of the crystalline phase (of also linear systems) of PLA, PCL and their mixed compositions has shown that the addition of polycaprolactone to PLA from 10 to 30% causes a sharp increase in the enthalpy of melting in this composition, and this is due to the plasticizing effect of finely dispersed particles of PCL. In the range of 50-70% PLA/PCL, apparently, there is a phase inversion, what leads to a sharp decrease in the enthalpy of melting. A further increase in the concentration of PCL in the mixture is accompanied by a sharp increase of ΔH in both polycaprolactone and PLA. Since the enthalpy of melting in the blended compositions with PCL content from 70 to 90 % is significantly lower than in the homopolymer, it can be assumed that interphase interlayers are formed in this material. A characteristic feature for these blended compositions is the decrease in the melting temperature of PLA as the concentration of PCL increases, starting from the composition 50/50 % from 170.5 to 165,1 ºC.

Sufficiently strong changes in the enthalpy of melting of the polymers under study should be accompanied by changes in the amorphous interlayers of fiber materials, what will be analyzed further using the EPR method.

 doi:10.20944/preprints202404.0063.v1

3.3. Dynamic Characteristics of the Amorphous Phase of Mixed PLA/PCL Compositions

In partially crystalline polymers, the structure of the amorphous regions is largely determined by the influence of their crystalline phase. Consequently, the mixing of crystalline PLA and PCL polymers changes not only the degree of crystallinity of the biopolyether, but also the molecular dynamics in the amorphous regions. To study the molecular/segmental mobility, we used an EPR method using the stable nitroxyl radical TEMPO, which acts as a molecular probe.

Let us consider the effect of the composition of the PLA/PCL mixture on the dynamics of the polymer molecules. It was shown earlier that the EPR spectra of the radical in PLA homopolymer matrices are a superposition of two spectra corresponding to two radical populations with their characteristic correlation times τ1 and τ2 [50–52]. Time τ1 reflects the mobility of molecules in denser amorphous regions with small free volume (the slow component of the spectrum), while τ2 reflects mobility in less dense regions with large free volume (the fast component of the same spectrum). The spectra for these polymers are shown in Figure 4.

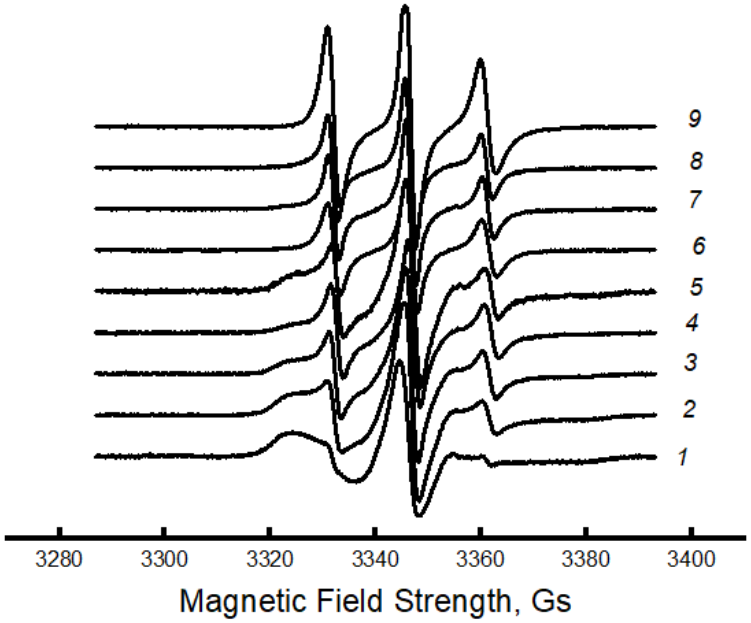

Figure 4. EPR spectra for PLA/PCL fibers: *1* – 100/0, *2* – 90/10, *3* – 80/70, *4* – 70/30, *5* – 50/50%, *6* – 70/30%, *7* – 80/20, *8* – 90/10, *9* – 0/100 %.

It can be seen that the spectra of PLA samples and PLA/PCL blended compositions with PLA content up to 70% look like a two-component system, i.e., there is an overlap of two spectra with slow and fast components. For samples with a PCL content of 70 % or more, the spectrum is single-component. The heterogeneous nature of the amorphous regions is due to the difference in the packing density of the polymer molecules and, therefore, to the different molecular dynamics. Because of their high potential barrier for internal rotation of chain links, PLA molecules are very rigid. The glassy dense mesh of this polymer prevents effective penetration of the radical, as confirmed by its low concentration in the samples (the radical was introduced at at 50 ºC). Using a special Simfonia and Winer program, concentrations of different density areas were evaluated. PCL has an elastic amorphous phase with high sorption properties. The amorphous phase of PLA is characterized by significantly higher correlation times and low radical concentration. As the PCL content in the mixture increases, the radical concentration increases dramatically (as shown in Figure. 5).

Preprints.org (www.preprints.org) | NOT PEER-REVIEWED | Posted: 2 April 2024 doi:10.20944/preprints202404.0063.v1

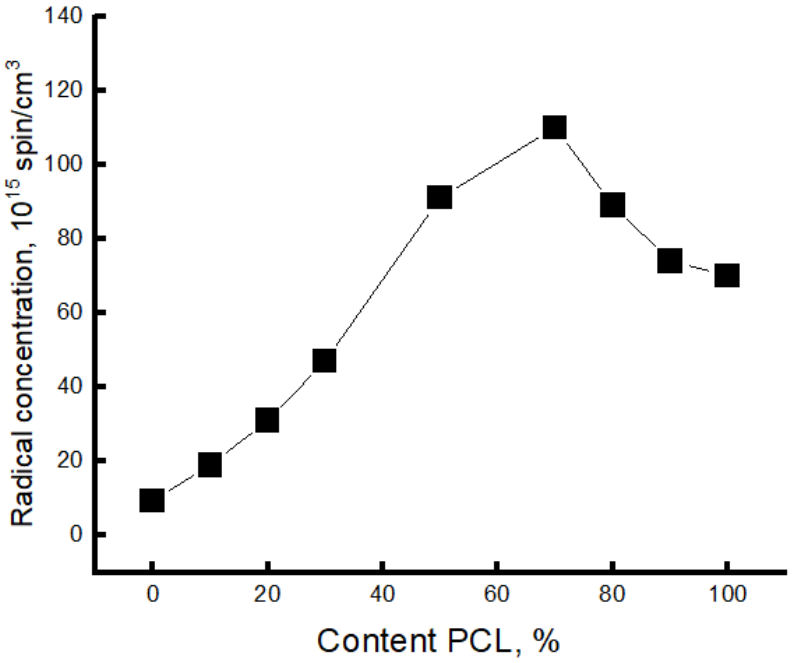

Figure 5. Changes in radical concentration from the composition of the PLA/PCL mixture.

It is in the region of 50-70% of the PCL content that a kink is observed in this dependence. As it was already shown in the previous section, the PCL concentration range of 50-70 % belongs to the phase inversion range, where practically all characteristics change their character depending on the composition, and a phase transition takes place when the dispersed phase of the PLA transforms into the dispersed phase.

Using mathematical processing of the experimental spectra using a special program Simfonia and Winer (Bruker®), the correlation times in PLA and PCL with different proportions in the mixture were calculated. Subtracting the spectrum of PCL from the spectra of the mixture composition, the correlation time τ1 in PLA was calculated (Figure 6a).

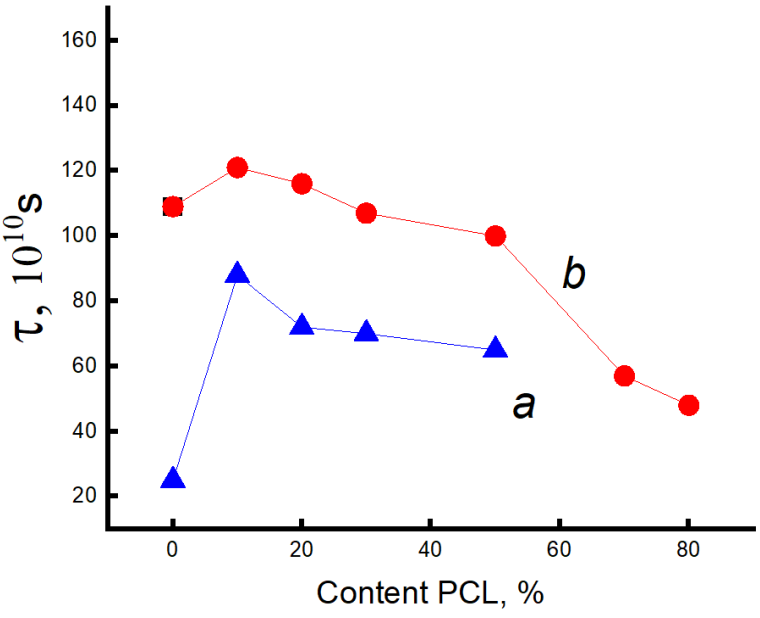

 doi:10.20944/preprints202404.0063.v1

Figure 6. Dependence of τ1 on the content of the composition when introducing the radical into the system at 50 ºC (**a**) and at 70 ºC (**b**).

The correlation time τ2 was calculated similarly (Figure 7a).

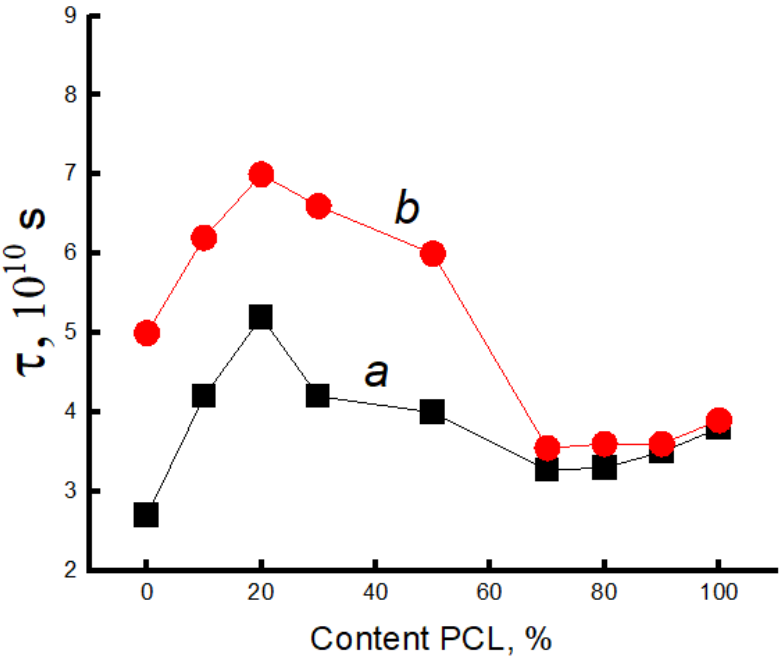

Figure 7. Dependence of τ2 on the content of the composition when introducing the radical into the system at 50 ºC (**a**) and at 70 ºC (**b**).

The figure shows that this parameter increases sharply (τ1 and τ2) when up to 20% PCL is introduced into the system, what suggests the presence of a transition of the amorphous structure of PLA from glassy to highly elastic state. The addition of up to 20% PCL causes its finely dispersed distribution in the system (as shown in [23]), what plasticizes the structure of the mixture and causes the growth of straightened macromolecules in the composition and, as a result, the molecular dynamics increases dramatically. In the concentration range from 20 to 50% PCL a decrease of τ1, τ2 is observed, what is caused by a decrease in the effect of plasticization of the structure by PCL particles due to an increase in their size [23]. At higher polycaprolactone concentrations in the mixture (from 50 to 70%), a kink is observed in the dependence of τ2 on the polymer composition, and further growth of the PCL concentration in the system leads to weak changes in the correlation time, despite a significant increase in the enthalpy of melting of this material. The growth of the share of crystalline regions and linear structures at the introduction of PCL of 70% or more should be accompanied by an increase in the share of straightened chains in the amorphous interlayers, but experimentally such changes in the compositions have not been recorded. It may be assumed that in the area of phase inversion the dispersed phase of PLA passes into a dispersion phase, the radical concentrates mainly in the amorphous structure of PCL due to the rather loose structure of this polymer (molecular mobility in it is almost 30 times higher than in PLA and the concentration of the radical is ~8 times higher). The radical provides information mainly on the molecular mobility of PCL at its concentration of more than 70%.

Since the melting temperature of PCL lies in the range 50-75 ºC, and the glass transition temperature of PLA in the range 60-75 ºC, the radical was introduced into the mixture compositions at two temperatures: 50 and 75 ºC.

Let us consider the dependences of correlation times on the mixture composition when the radical is introduced into the fiber at 75 ºC. Correlation times were calculated similarly to the previous

 doi:10.20944/preprints202404.0063.v1

experiment. Figure 6b and 7b show the dependences of the characteristic correlation time for the fast and slow components of the EPR spectrum on the mixture composition. It can be seen that with the introduction of the radical at 75 ºC the character of the dependences did not change, only higher values of τ were realized in the fibers with the composition from 0 to 50% PCL due to the accessibility for the radical of denser amorphous regions of the material. At a higher content of this polymer in the mixture, from 50 to 70%, a kink in the dependence τ on the composition of the composition was also observed. When the concentration of PCL in the mixture is higher than 70%, the molecular dynamics in the amorphous regions slows down insignificantly.

The nature of the dependencies of the correlation time on the mixture composition when the radical is added at 75 ºC differs only by higher values of τ1 and τ2 in the region with high PLA content (up to 50%) than when it is added at 50 ºC. At addition of more than 70 % PCL the curves coincide irrespective of the temperature of introduction of the radical.

Thus, the patterns of changes in the molecular dynamics in PLA/PCL fiber material are similar to the changes in the enthalpy of melting of this polymer, thus confirming the conclusion about the plasticizing effect of adding PCL up to 50%. At its small concentrations (up to 30%) the distribution of PCL occurs in the form of tiny particles, and perhaps they are also the germs of crystallization. In this case, the possibility for sufficiently straightened macromolecules to adopt the maximally straightened conformation and create additional crystalline and linear structures is realized (as confirmed by DSC data) and, as a result, ΔH τ_1 and τ_2 greatly increase. The observed changes can be explained by the transformation of the amorphous structure from glassy to highly elastic state. A further increase in the concentration of PCL in the system leads to an increase in the size of the PCL particles (according to the literature data) and the plasticization effect of the structure of the mixture composition decreases, a decrease in the dynamic and structural parameters is observed. In the region of compositions of 50-70% PLA/PCL a kink is observed in the dependencies of ΔH τ_1 and τ_2 on the composition, what is explained by the phase inversion in the mixture composition. At the PLA content of 70% the PCL becomes a continuous phase, the melting enthalpy of both PLA and PCL begins to increase significantly, but the correlation time increases insignificantly, what can be explained by weak changes in the amorphous regions of PCL. Regardless of the temperature of introduction of the radical into the PLA/PCL system, the character of the change in the correlation time from the mixture composition does not change (Figures 6 and 7). When the radical is introduced at 75 ºC, τ1 and τ2 are characterized by higher values in comparison with these parameters obtained at 50 ºC only in the region of PCL concentrations less than 70%. At a higher concentration of PCL in the system, regardless of the temperature of introduction of the radical, these curves coincide.

The fraction of sorbed probe increases significantly with increasing PCL concentration in the material and in the region of 50-70 % PCL a kink occurs due to the formation of a much softer continuous PCL structure. At a higher addition of this material, the concentration decreases.

The closeness of the form of concentration curves, melting enthalpy, correlation time, reflecting the structural and dynamic nature of the polymer mixture, is determined by its phase transformation, namely, by the transition of PLA from dispersed material into a dispersion medium.

Additional information on the dynamic behavior of the PLA/PCL system of different compositions was obtained by studying the temperature dependence of the rotation speed of the molecular probe (Figure 8).

Preprints.org (www.preprints.org) | NOT PEER-REVIEWED | Posted: 2 April 2024 doi:10.20944/preprints202404.0063.v1

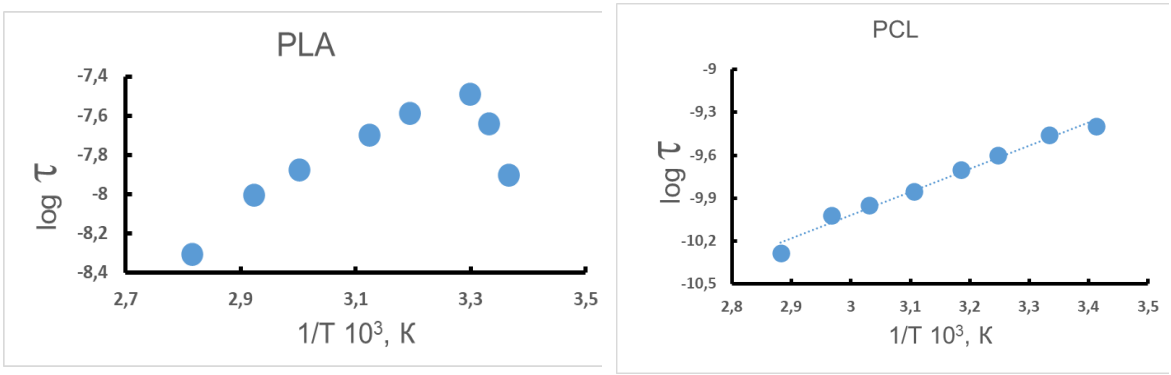

(**a**) (**b**)

Figure 8. Temperature dependence of τ2 in PLA (**a**) and in PCL (**b**) (radical introduced at 50 ºC).

In PLA homopolymer, the segmental dynamics decreases when the sample is heated to 40 ºC, indicating the heterogeneous structure of this polymer. During the heating, owing to heterogeneity of PLA, its intercrystalline structures are progressively involved into molecular transformation and the denser regions are getting accessible for TEMPO radical penetration with the retardant of its mobility. At higher temperatures (over 40 ºC) mobility begins to increase (Figure 8). In mixtures with the addition of PCL up to 50%, the temperature dependence of the correlation time has a kink at temperatures of 40-50 ºC. In fibers with PCL content of 70 % and more, this dependence has a linear character, what indicates a homogeneous structure in which the radical is sorbed.

The effective activation energies Eτ, (Figure 9) were calculated for the fast component when the radical was introduced at 70 ºC.

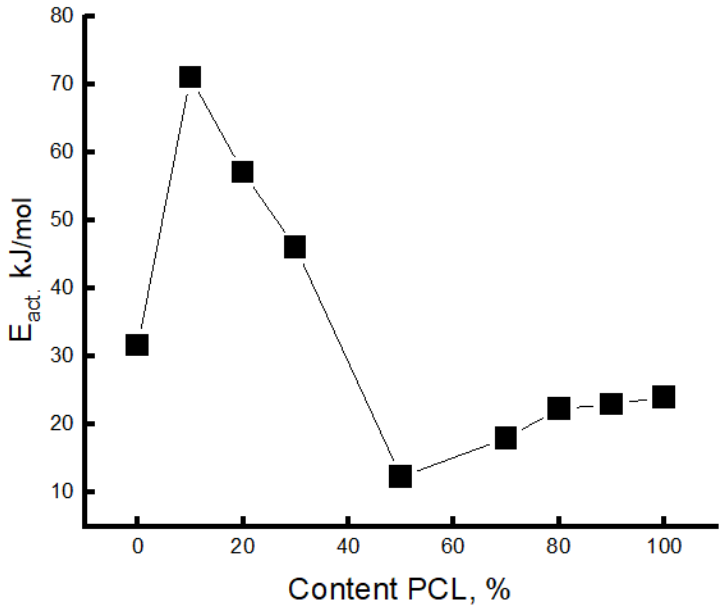

Figure 9. Change in activation energy depending on the composition of the mixture.

The values of Eτ decrease with increasing PCL concentration in the system and in the region of 50/50 and 70/30 % concentrations are characterized by ~~rather~~ the lowest values (the region of phase inversion). At higher PCL concentrations in the system, the Eτ values are slightly increased. The obtained result also confirms the conclusion about the presence of phase inversion in the region of PCL concentration 50-70%, what corresponds to all previous results.

 doi:10.20944/preprints202404.0063.v1

4. Conclusions

The study of PLA/PCL composites in fibrillar state at thermal (DSC) and spectral (EPR) levels allowed the authors to analyze the effect of constituent composition on the structural and dynamic characteristics.

A sharp increase in the enthalpy of melting and molecular dynamics in the above binary system with the addition of 10% PCL was revealed, which is due to the finely dispersed distribution of this polymer in the PLA matrix and its plasticizing effect on the structure of polylactide. As a result of plasticizing, segmental dynamics enhances and the proportion of straightened chains in the PLA fiber increases. With increasing the PCL content up to 70% values of ΔH and τ have the trend to decrease, indicating the formation of PLA dispersive phase. At the same time the plasticizing effect of PCL on the structure of PLA decreases owing to the reduce in the number of PCL-PLA segmental contacts. The changes in thermal characteristics and molecular dynamics of the binary PLA/PCL system depending on its composition allowed the authors to identify a specific ~~area~~ interval of concentration, from 50/50 to 70/30%, where the phase inversion occurs, namely, the process of transformation of continuous dispersion medium of PLA into dispersive phase. Here, the melting enthalpy, and correlation time ~~is~~ are characterized by relatively low values and only starting from 70% of PCL content in the system ΔH significantly increases. Molecular dynamics slows down insignificantly, since changes in the proportion of crystalline and linear structures in the system do not have a significant effect on the amorphous component. The concentration of the radical in PLA is low due to its crystallinity and high molecular rigidity compared to the molecular dynamics of PCL.

Author Contributions: conceptualization, A.A.O., S.G.K., A.L.I; research, I.A., S.G., A.A., O.I., A.A., and A.V.; resources, I.A.; data supervision, S.G.; writing - preparation of original draft, S.G. and A.A.; writing - reviewing and editing, A.A., I.A.V, and O.I.,; visualization, S.G.; author supervision, S.G. A.L.I; project management, I.A.; fundraising, A.L.I. All authors have read and agreed to the published version of the manuscript.

Funding: This study did not receive external funding.

Data Availability Statement: Not applicable.

Acknowledgments: The authors express a profound appreciation for PHB providing to Dr. U. Haenggi (Biomer Company) and the Biomer company. DSC crystallinity measurements were performed at the RUDN University. The study was carried out using scientific equipment of the Center of Shared Usage «New Materials and Technologies» of Emanuel Institute of Biochemical Physics

Conflicts of Interest: The authors declare no conflict of interest.

References

1. P. C. Pires, F. Mascarenhas-Melo, K. Pedrosa, et al. Polymer-based biomaterials for pharmaceutical and biomedical applications: A focus on topical drug administration. *European Polymer Journal*. **2023**. *187*, 111868. https://doi.org/10.1016/j.eurpolymj.2023.111868
2. R. Pugliese, B. Beltrami, S. Regondi, C. Lunetta. Polymeric biomaterials for 3D printing in medicine: An overview. *Annals of 3D Printed Medicine* **2021**. *2*, 100011. https://doi.org/10.1016/j.stlm.2021.100011
3. N. Singh, O. A. Ogunseitan, M. H. Wong, Y. Tang. Sustainable materials alternative to petrochemical plastics pollution: A review analysis. *Sustainable Horizons* **2022**. *2*, 100016. https://doi.org/10.1016/j.horiz.2022.100016
4. Z. Zhang, S. Zou, P. Li. Aging of plastics in aquatic environments: Pathways, environmental behavior, ecological impacts, analyses and quantifications. *Environmental Pollution* **2024**. *341*, 122926. https://doi.org/10.1016/j.envpol.2023.122926
5. Q. Chen, R. Auras, I. Uysal-Unalan. Role of stereocomplex in advancing mass transport and thermomechanical properties of polylactide. *Green Chemistry* **2022**. *24* (9), 3416-3432 https://doi.org/10.1039/d1gc04520b
6. S. S. Ray, R. Banerjee. Introduction: sustainability, polylactide and polylactide-based composites. *Sustainable Polylactide-Based Composites*. **2023**. 1-24. https://doi.org/10.1016/B978-0-323-99640-2.00004-0
7. A. K. Aworinde, S. O. Adeosun, F. A. Oyawale et al. Comprehensive data on the mechanical properties and biodegradation profile of polylactide composites developed for hard tissue repairs. *Data in Brief*. **2020**. *32*, 106107. https://doi.org/10.1016/j.dib.2020.106107

8. T. Patrício, A. Glória, and P. Bártolo. Mechanical and biological behaviour of PCL and PCL/PLA scaffolds for tissue engineering applications. *Chem. Eng. Trans.* **2013.** *32*, 1645–1650. https://doi.org/10.3303/CET1332275.
9. M. Todo, S.-D. Park, T. Takayama, and K. Arakawa. Fracture microme-chanisms of bioabsorbable PLA/PCL polymer blends. Eng. Frac. Mech. 2007, 74, 1872–1883. https://doi.org/10.1016/j.engfracmech.2006.05.021.
10. R. Auras, L.T. Lim, S.E.M. Selke, and H. Tsuji. Optical Properties. In 'Poly (lactic acid): synthesis, structures, properties, processing, and applications'. *Hoboken, NJ: John Wiley & Sons,* **2010.** 113–124. https://doi.org/10.1002/9780470649848.ch8.
11. L. Fambri, and C. Migliaresi. Crystallization and thermal properties, in Poly(lactic acid): Synthesis, Structures, Properties, Processing, and Applications, **2022.** Chapter 8. https://doi.org/10.1002/9780470649848.ch9.
12. S. Krishnan, P. Pandey, S. Mohanty, and S. K. Nayak. Toughening of poly-lactic acid: an overview of research progress. *Polym.-Plast. Technol. Eng*. **2016**. *55*, 1623–1652. https://doi.org/10.1080/03602559.2015.1098698.
13. T.C. Yang. Effect of extrusion temperature on the physico-mechanical properties of unidirectional wood fiber-reinforced polylactic acid composite (WFRPC) components using fused depositionmodeling. *Polymers.* **2018**. *10,* 976. https://doi.org/10.3390/polym10090976.
14. J.R. Porter, T.T. Ruckh, T.T. and K.C. Popat. Bone tissue engineering: A review in bone biomimetics and drug delivery strategies. *Biotechnol. Prog.,* **2009**. *25* (6), *1539–1560.* https://doi.org/10.1002/btpr.246.
15. M. Vert. Degradable and bioresorbable polymers in surgery and in pharma-cology: beliefs and facts. *Journal of Materials Science: Materials in Medicine*. **2009**. *20*, 437-446.
16. R. Dwivedi, S. Kumar, R. Pandey, A. Mahajan, D. Nandana, D.S Katti, D. Mehrotra. Polycaprolactone as biomaterial for bone scaffolds: Review of literature. *Journal of Oral Biology and Craniofacial Research*. **2020**. *10* (1), 381-388. https://doi.org/10.1016/j.jobcr.2019.10.003.
17. S. Wachirahuttapong, C. Thongpin, N. Sombatsompop. Effect of PCL and Compatibility Contents on the Morphology, Crystallization and Mechanical Properties of PLA/PCL Blends. *Energy Procedia.* **2016.** *89*, 198-206. doi:10.1016/j.egypro.2016.05.026
18. A.K. Matta, R. Umamaheswara, K.N.S. Suman, V. Rambabu. Preparation and Characterization of Biodegradable PLA/PCL Polymeric Blends. *Procedia Materials Science*. **2014**, *6*, 1266-1270. doi:10.1016/j.mspro.2014.07.201
19. A. Merkli, C. Tabatabay, R. Gurny, J. Heller. Biodegradable polymers for the controlled release of ocular drugs. *Progress in Polymer Science*. **1998**, *23* (3) 563-580. https://doi.org/10.1016/S0079-6700(97)00048-8.
20. S. Freiberg, X. Zhu. Polymer microspheres for controlled drug release. *International Journal of Pharmaceutics.* **2004,** *282* (1-2), 1-18. https://doi.org/10.1016/j.ijpharm.2004.04.013.
21. I. Fortelny, A. Ujcic, L. Fambri, M. Slouf. Phase Structure, Compatibility, and Toughness of PLA/PCL Blends: A Review. *Front. Mater. Sec. Polymeric and Composite Materials.* **2019**. *6* (1–13); https://doi.org/10.3389/fmats.2019.00206. This article is part of the Research Topic Biodegradable Matrices and Composites.
22. N. López-Rodríguez A. López-Arraiza, E. Meaurio, J.R. Sarasua. Crystallization, morphology, and mechanical behavior of polylactide/poly(ε-caprolactone) blends. *Polymer Engineering & Science.* **2006.** *46* (9), 1131-1332. https://doi.org/10.1002/pen.20609.
23. V. Mittal, T.Akhatar, G. Luckachan, and N. Matsko. PLA, TPS and PCL binary and ternary blends: structural characterization and time-dependent morp-hological changes. *Colloid Polymer Science*, **2015**, *293*, 573–585.
24. V. Mittal, T.Akhatar, G. Luckachan, and N. Matsko. Synergistic effects in mechanical properties of PLA/PCL blends with optimized composition, proces-sing, and morphology. *Mater. Eng.*, **2015**, *300*, 423–435. https://doi.org/10.1039/C5RA21178F.
25. J. Urquijo, G. Guerrica-Echavarria, and J. I. Equiazabal. Melt processed PLA/PCL blends: Effect of processing method on phase structure, morphology, and mechanical properties. *Journal of Applied Polymer Science*, **2015**, 132, 42641. https://doi.org/10.1002/app.42641.
26. M. Delgado-Aguilar, R. Puig, I. Sazdovski, and P. Fullana-i-Palmer. Poly-lactic Acid/Polycaprolactone Blends: On the Path to Circular Economy, Substi-tuting Single-Use Commodity Plastic Products. *Materials (Basel).* **2020**, *13* (11), 1-18. https://doi.org/10.3390/ma13112655.
27. A.K. Matta, R. Umamaheswara, K.N.S. Suman, V. Rambabu. Preparation and Characterization of Biodegradable PLA/PCL Polymeric Blends. *Procedia Materials Science.* **2014,** *6*, 1266-1270. https://doi.org/10.1016/j.mspro.2014.07.201.
28. A. Ostafinska, I. Fortelny, M. Nemoral, J. Hodan, J. Kredatusova, and M. Slouf. Synergistic effects in mechanical properties of PLA/PCL blends with op-timized composition, processing, and morphology. RSC Advances. 2015, 5, 98971-98982. https://doi.org/10.1039/c5ra21178f.
29. J.-M. Raquez, S. Vanderstappen, F. Meyer, P. Verge, M. Alexandre, J.-M. Thomassin, C. Jérôme, P. Dubois. Design of Cross-Linked Semicrystalline Poly(ε-caprolactone)-Based Networks with One-Way and Two-

 doi:10.20944/preprints202404.0063.v1

Way Shape-Memory Properties through Diels–Alder Reactions. *Chemistry–A European Journal*. **2011**, *17* (36), 10135-10143. https://doi.org/10.1002/chem.201100496.

30. M.D. Hager, M. D.; S. Bode, C. Weber, U.S. Schubert. Shape memory polymers: Past, present and future developments. *Progress in Polymer Science*. **2015,** *49–50,* 3-33. https://doi.org/10.1016/j.progpolymsci.
31. H. Rodríguez-Tobías, G. Morales, A. Ledezma, J. Romeso, R. Saldivas, V. Langlois. Electrospinning and electrospraying techniques for designing novel antibacterial poly (3-hydroxybutyrate)/zinc oxide nanofibrous composites. *J. Mater. Sci*. **2016**, *51* (18), 8593-8612. https://doi.org/10.1016/j.msec.2014.01.046.
32. A.L. Iordanskii, A.A. Ol'khov, S.G. Karpova, E.L. Kucherenko, R.Yu. Kosenko, S.Z. Rogovina, A.E. Chalykh, A.A. Berlin. Influence of the structure and morphology of ultrathin poly (3-hydroxybutyrate) fibers on the diffusion kinetics and transport of drugs. *Polymer Science. A.* **2017**, *59*, (3), 343. https://doi.org/ 10.1134/S0965545X17030075.
33. S.G. Karpova, A.A. Ol'khov, A.L. Iordanskii, S.M. Lomakin, N.S. Shilkina, A.A. Popov, K.Z. Gumargalieva, and A.A. Berlin. Nonwoven blend composites based on poly (3-hydroxybutyrate)–chitosan ultrathin fibers prepared via electrospinning. *Polymer Science. A.* **2016**, *58* (1), 76-87. https://doi.org/10.7868/S2308112016010041.
34. D.F. Parra, D.S. Rosa, J. Rezende, P. Pous, A.B. Lugao. Biodegradation of γ irradiated poly 3-hydroxybutyrate (PHB) films blended with poly (Ethyleneglycol). *J. Polym. Environment*. **2011**, *19* (4), 918-932. https://doi.org/10.1007/s10924-011-0353-x.
35. T.C. Yang. Effect of extrusion temperature on the physico-mechanical properties of unidirectional wood fiber-reinforced polylactic acid composite (WFRPC) compo-nents using fused depositionmodeling. Polymers. 2018,10, 976. https://doi.org/10.3390/polym10090976.
36. J.R. Porter, J.R. Ruckh, and K.C. Popat. Bone tissue engineering: A review in bone biomimetics and drug delivery strategies. Biotechnol. Prog., 2009, 25 (6), 1539–1560. https://doi.org/10.1002/btpr.246.
37. M. Vert. Degradable and bioresorbable polymers in surgery and in phar-ma-cology: beliefs and facts. Journal of Materials Science: Materials in Medicine, 20 2009, 20, 437-446. https://doi.org/10.1007/s10856-008-3581-4.
38. R. Dwivedi, S. Kumar, R. Pandey, A. Mahajan, D. Nandana, D.S. Katti, D. Mehrotra. Polycaprolactone as biomaterial for bone scaffolds: Review of literature. Journal of Oral Biology and Craniofacial Research. 2020, 10 (1), 381-388. https://doi.org/10.1016/j.jobcr.2019.10.003.
39. S. Freiberg, X. Zhu. Polymer microspheres for controlled drug release. Inter-national Journal of Pharmaceutics. 2004, 282 (1-2), 1-18. https://doi.org/10.1016/j.ijpharm.2004.04.013.
40. I. Fortelny, A. Ujcic, L. Fambri, M. Slouf. Phase Structure, Compatibility, and Toughness of PLA/PCL Blends: A Review. Front. Mater. Sec. Polymeric and Composite Materials. 2019, 6 (1–13). https://doi.org/10.3389/fmats.2019.00206. This article is part of the Re-search Topic Biodegradable Matrices and Composites.
41. N. López-Rodríguez, A. López-Arraiza, E. Meaurio, J.R. Sarasua. Crystalliza-tion, morphology, and mechanical behavior of polylactide/poly(ε-caprolactone) blends. Polymer Engineering & Science. 2006, 46 (9), 1131-1332. https://doi.org/10.1002/pen.20609.
42. 40. V. Mittal, T. Akhatar, G. Luckachan, and N. Matsko. PLA, TPS and PCL bi-nary and ternary blends: structural characterization and time-dependent morp-hological changes. Colloid Polymer Science, 2015, 293, 573–585. https://doi.org/10.1007/s00396-014-3458-7.
43. Y.N. Filatov. Electroforming of fibrous materials (EFV-process). Moscow: Oil and Gas, **1997**.
44. D.E. Budil, S. Lee, S. Saxena, J.H Freed. Nonlinear-Least-Squares Analysis of Slow-Motion EPR Spectra in One and Two Dimensions Using a Modified Levenberg–Marquardt Algorithm. *Journal of Magnetic Resonance, Series A.* **1996**, *120*, (2), 155-189. https://doi.org/10.1006/jmra.1996.011.
45. V.P. Timofeev, A.Yu. Misharin, Y.V. Tkachev. Biophys. 2011, 56 (3), 420.
46. A.L. Buchachenko, A.M. Wasserman. Stable radicals. Moscow: Chemistry, **1973.**
47. K. Bule Možar, M. Miloloža V. Martinjak, M. Cvetnić H. Kušić, T. Bolanča, D. Kučić Grgić. Potential of Advanced Oxidation as Pretreatment for Microplastics Biodegradation. Separations. *Faculty of Chemical Engineering and Technology, University of Zagreb*. **2023**, *10* (2), 132; (Marulićev Trg 19, 10000 Zagreb, Croatia). https://doi.org/10.3390/separations10020132.
48. A.A. Olkhov, S.G. Karpova, P.M. Tyubaeva, A. Zhulkina, Yu.N. Zernova, A.L. Iordanskii. Effect of Ozone and Ultraviolet Radiation on Structure of Fibrous Materials Based on Poly(3-hydroxybutyrate) and Polylactide. *Inorganic Materials: Applied Research.* **2020**, *11*(5), 1130-1136. https://doi.org/10.1134/S2075113320050251.
49. F. Kucera, J. Petrusa, J. Jancara. The structure-hydrolysis relationship of poly(3-hydroxybutyrate). *Polymer Testing*. **2019**, *80*, 106095. https://doi.org/10.1016/j.polymertesting.2019.106095.
50. P. Klonos, Z. Terzopoulou, S. Koutsoumpis, P. Pissis. Rigid amorphous fraction and segmental dynamics in nanocomposites based on poly(L–lactic acid) and nano-inclusions of 1-3D geometry. *European Polymer Journal.* **2016,** *82*, 16–34. https://doi.org/10.1016/j.eurpolymj.2016.07.002.

 doi:10.20944/preprints202404.0063.v1

51. 49. P.P. Kamaev, I.I. Aliev, A.L. Iordanskii, A.M. Wasserman. Molecular dynamics of the spin probes in dry and wet poly(3-hydroxybutyrate) films with different morphology. *Polymer.* **2001**, *42* (2), 515–520. https://doi.org/10.1016/S0032-3861(00)00339-6.
52. O. Staroverova S. Karpova, A. Iordanskii, A. Olkhov, A. Khvatov, A. M. Grumezescu, N. Kildeeva, M. Artsis, G. Zaikov. Comparative Dynamic Characteristics of Electrospun Ultrathin Fibers and Films Based on Poly(3-hydroxybutyrate). *Chemistry & Chemistry Technology*. **2016**, *10* (2), 151-157. https://doi.org/10.23939/chcht10.02.151.